JCBPS; Section A; May 2018 – July - 2018, Vol. 8, No. 3; 377-391. E- ISSN: 2249 –1929
[DOI: 10.24214/jcbps.A.8.3.37791]

Journal of Chemical, Biological and Physical Sciences

An International Peer Review E-3 Journal of Sciences

*Available online at*www.jcbsc.org

Section A: Chemical Sciences

CODEN (USA): JCBPAT Research Article

Ferula Hermonis (FH) extract as a green inhibitor for resisting corrosion of stainless steel 430in hydrochloric acid solution

A.S.Fouda, H. A. Mostafa, A. F. S. Molouk, H .M. El-Saeed

Chemistry Department, Faculty of Science, Mansoura University, Mansoura-35516, Egypt,

Received: 26 May 2018; **Revised:** 08 June 2018; **Accepted:** 16 June 2018

Abstract: The inhibiting influence of ferula hermonis (FH) towards the corrosion performance of stainless steel 430 (SS430) in 2.0 M HCl was planned utilizing mass reduction (MR), potentiodynamic polarization (PP), AC impedance spectroscopy (EIS) and electrochemical frequency modulation (EFM) tests. The hindrance efficiency of the extract improved with rising the dose of extract and decreases with temperature rising. The parameters obtained from thermodynamic due to corrosion and adsorption procedures have measured and debated. The adsorption of (FH) on the SS 430 surface in HCl has got to follow Langmuir isotherm. PP showed that (FH) extract plays as a mixed kind inhibitor. (EIS) data correlated with potentiodynamic polarization results. The surface tests of protected SS 430 were examined by scanning electron microscope (SEM), atomic force microscopy (AFM), and Fourier transform infrared (FT-IR).

Keywords: SS430, Corrosion inhibition, HCl, Ferula Hermonis (FH) extract

1. INTRODUCTION

The corrosion of SS is very significant, and requires proper attention from scientists to avoid economical loss. SS430 is one of the most used ferretic grades of SS, it found in interior appliances like washing machine drums, kitchen sinks, dishwasher, indoor parries and cooking utensil. Because of high chromium content in grade 430 it forms renewable protective layer, this protective layer was disappeared in the presence of acidic medium[1,2]. Therefore, using of corrosion inhibitors is efficient, economic, and recognized method for preventing or slowing down the MR and acid consumption rate [3-5]. In the last 10 years the researchers' attention by utilizing corrosion hindrance established on

the plant extract due to inexpensive, readily accessible and renewable sources of materials[6]. There are numerous literature surveys of plant extracts which act as beneficial corrosion hindrance with high efficiency. Study done by Saxena used Butea monosperma which shows 98% hindrance proficiency[7] at 500 mg/L. Radish seeds give 79% protection, productivity[8] at 10 mg/L. Leaves of Juniperus procera, which investigated for carbon steel in 1M HCl gives inhibition[9], reached 85%. Anise Extract which has inhibited[10] reached to 93% at 400 ppm. Using curcumin, parsley and cassia bark extracts at 500 ppm give inhibition[11] more than 80%. The ethanol extract of propolis[12] gives %IE reached to 95%. Mentha spicata L Extract at optimum concentration 250 ppm showed 96% inhibition efficiency[13]. Terminalia ivorensis also showed a high corrosion inhibition[14] *ca.* 89.5%. So from all previous surveys, plant extract has the priority to be used. In the present work we use plant extract named Ferula hermonis (FH) in the family of apiaceae with common name zallouh or Lebanese Viagra it is very available, and grow widely in the Mediterranean region. The Aim of this investigation is studying the influence of FH extract as eco-friendly corrosion inhibitor for the SS430 corrosion in 2M HCl utilizing electrochemical and non-electrochemical tests. The morphology of the surface was studied using atomic force microscopy (AFM), scanning electron microscope (SEM), and (FTIR)

2. EXPERIMENTAL

2.1 Material planning : The chemical conformation of SS 430 present in this study is C 0.12%, P 0.045%, Si 1.0%, S 0.03%, Mn 1.0%, Ni 0.05%, Cr 16%, and Fe which represents the rest of the weigh percentage. The SS430 specimens were cut with dimensions 2 x 1.9 x 0.2 cm for MR measurements and 1 x 1 x 0.2 cm for electrochemical techniques with showing surface area 1cm^2. These specimens were polished with emery paper 1000, 1500 and 2000 to a metallic shine. The tested 2M HCl was prepared by diluting analytical 34% HCl with bidistilled water.

Plant extract preparation occurred through collecting Ferula Hermonis leaves from the Sadat city desert, Egypt. This leaf, washed, dried at room temperature and coarsely crushed in a cylindrical crusher to obtain a fine powder. In order to get the extract 200g of leaf powder submerged in 70% methanol for 48 hr the powder was removed by filtration to get clear filtrate after that, the filtrate was vaporized under vacuum; the residue was collected and stored in refrigeration. The concentration of used inhibitor ranged from (50-300) ppm. FH extract consists of Ferutinin, Teferin, and Teferidin.

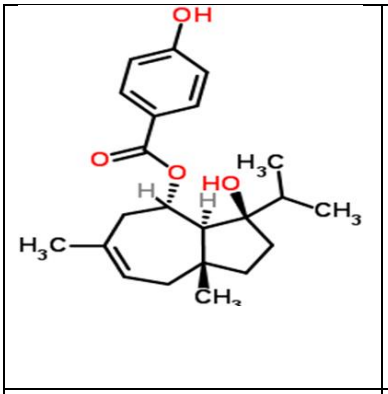	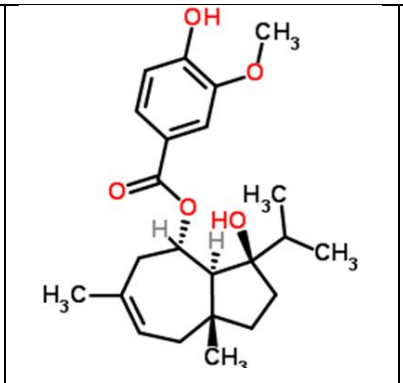	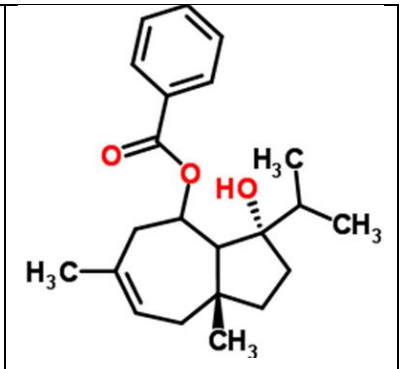
Ferutinin	Teferin	Teferidin

2.2 MR tests: The pretreated SS430 coins have dipped in 100 mL of 2 M HCl solution without and with various concentrations of FH extract at 25°C, 30°C, 35°C, 40°C and 45°C for 3h after designated

time, the SS430 coins have obtained from the aggressive solution, dipped with bidistilled water, dried and weighed.

2.3 Electrochemical techniques: The electrochemical tests were achieved by utilizing a three-electrode cell, linked to (Potentiostat /Galvanostat (Gamry PCI 300/4). For fitting data, we use Gamry Echem analyst 6.03 software. The cell consists of reference electrode (SCE), counter electrode (Pt) and SS430 as a working electrode in a glass vessel of capacity 100 ml. The working electrode was prepared as follows at first one side of SS430 sheet (10 mm x 10 mm x 2 mm) was welded to a Cu wire. The Cu wire attached with SS430 was inserted into a glass tube and SS430 exposed to the test solutions is 1 cm^2. All tests were obtained at 25°C.PP were obtained by exchange the electrode potential from -500 to 500 mV vs. open circuit potential (OCP) with scan rate 1 mVs^{-1}. EIS test was accepted in a frequency range from 0.1 Hz to 10^{-5} Hz with amplitude of 10 mV under open circuit condition. EFM technique performed using two frequencies (2.0–5.0 Hz). The greater band utilized to measure the corrosion parameters. The experiments were performed after immersing the electrode for 30 min in order to reach the steady state.

2.4 Surface characterization: Analysis of SS430 surface taken without and with optimum dose 300 ppm of the FH extract after immersing them in 2M HCl for 15h. After immersion period the specimens washed by bidistilled water, dried, and then examined the tests were achieved utilizing SEM (JOEL 840, Japan), and atomic force microscope (AFM), while for FTIR analyses SS430 surface was examined after immersion 3h in 300 ppm of FH extract and compared to the spectra of FH extract.

3. RESULT AND DISCUSSION

3.1 MR tests: MR of SS430 in 2M HCl was obtained at different time intervals without and with (50-300) ppm FH extract at 25°C as shown in **Fig.1.**

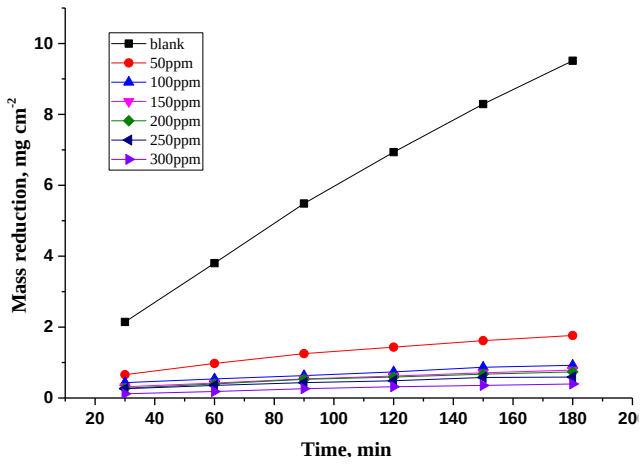

Figure (1): Time - MR diagrams of SS 430 in 2 M HCl without and with various doses of FH extract at 25° C

It can be observed that MR decreases as the dose of extract rises. The %IE measured from the equation (1).

$$\%IE = \theta \times 100 = \frac{k_{corr} - k_{corr\,(inh)}}{k_{corr}} \times 100 \quad (1)$$

Where, k_{corr} and $k_{corr(inh)}$ are the data on corrosion rates (mg $cm^{-2}min^{-1}$) without and with FH extract, correspondingly. The values of k_{corr}, %IE, and θ were summarized in **Table (1)**

Table 1: Effect of temperature on k_{corr} and % IE through MR measurements at different temperatures after 120 min immersion

Temp., *°C*	[inh], *ppm*	k_{corr}, *mg* cm^{-2} *min*$^{-1}$	Ɵ	% IE
25	Blank	0.058	-	-
	50	0.012	0.793	79.3
	100	0.006	0.896	89.6
	150	0.0052	0.910	91
	200	0.005	0.914	91.4
	250	0.0041	0.929	92.9
	300	0.003	0.948	94.8
30	Blank	0.124	---	---
	50	0.028	0.774	77.4
	100	0.017	0.862	86.2
	150	0.0132	0.893	89.3
	200	0.011	0.911	91.1
	250	0.0095	0.923	92.3
	300	0.007	0.943	94.3
35	Blank	0.19	---	---
	50	0.0447	0.764	76.4
	100	0.034	0.821	82.1
	150	0.0241	0.873	87.3
	200	0.02	0.895	89.5
	250	0.0182	0.904	90.4
	300	0.015	0.921	92.1
40	Blank	0.225	---	---
	50	0.0844	0.625	62.5
	100	0.056	0.751	75.1
	150	0.038	0.831	83.1
	200	0.036	0.84	84
	250	0.0332	0.852	85.2
	300	0.025	0.888	88.8
45	Blank	0.38	---	---
	50	0.178	0.532	53.2
	100	0.151	0.603	60.3
	150	0.0851	0.776	77.6
	200	0.079	0.792	79.2
	250	0.0627	0.835	83.5
	300	0.047	0.876	87.6

The ending data of %IE improve by raising the extract dose and reached 94.8% at optimum concentration 300ppm at 25°C, while the effect of temperature showed lower in protection efficiency with rising temperature this can be regarded to desorption of FH extract from SS430 surface

3.2 Adsorption isotherms: The relation between surface coverage and concentration of FH extract was confirmed diagrammatically by fitting to various adsorption isotherms. The best fit was found to obey Langmuir isotherm (Eq. 2) with a high correlation coefficient (R^2) see **Fig (2).**

$$K_{ads}\, C = \frac{\theta}{1-\theta} \qquad (2)$$

Where C is the dose (g L^{-1}) of the FH extract in the bulk electrolyte and K_{ads} is the adsorption equilibrium constant. The standard free energy of adsorption (ΔG^{o}_{ads}), can be determined by:

$$K_{ads} = \frac{1}{55.5}\, exp\,[-\Delta G^{\circ}_{ads} / RT] \qquad (3)$$

Where 55.5 is the molar dose of water in the solution in M^{-1}. Thermodynamic parameters for the adsorption of the FH extract on SS 430 surface in 2 M HCl at various temperatures was recorded in **Table (2).** The –ve sign of ΔG°_{ads} indicate the spontaneity of process and the constancy of the adsorbed layer[15] on the surface of SS 430. If the values of ΔG°_{ads} are around -20 kJ mol^{-1} or lesser, this designates the electrostatic interaction between charged SS430 surface and charged organic molecules obtained from FH extract in the bulk of the solution[16]. The ΔH°_{ads} has a negative sign indicates that the process is exothermic. Mostly, it is known that if the enthalpy values less than 40kJmol^{-1} the adsorption process is due to the electrostatic interactions among charged molecules obtained from FH extract and charged SS grade 430 that suggest physical adsorption process[17].

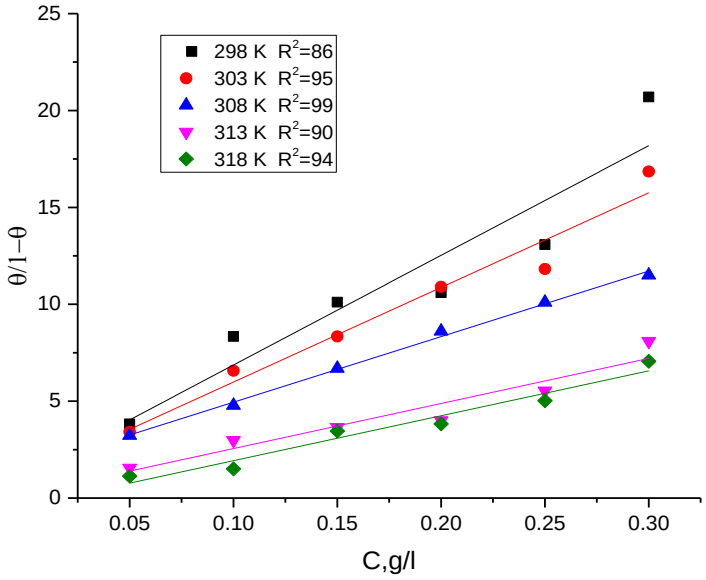

Fig (2): Langmuir Adsorption isotherm curves as θ/1- θ &C of the adsorption of Ferula hermonis extract on SS 430 in 2M HCl at various temperature

Table (2): Adsorption data of SS430 in 2M HCl and FH extract by Langmuir isotherm at dissimilar temperatures

Inhibitor	T, *K*	Log k_{ads}, M^{-1}	$-\Delta G^{\circ}_{ads}$ *kJ mol*$^{-1}$	$-\Delta H^{\circ}_{ads}$ *kJ mol*$^{-1}$	$-\Delta S^{\circ}_{ads}$ *J mol*$^{-1}$ *K*$^{-1}$
Ferula hermonis	298	1.75	19.95	39	197.8
	303	1.69	19.92		194.5
	308	1.53	19.3		189.3
	313	1.37	18.65		184.2
	318	1.36	18.93		182.2

3.3 Kinetic and thermodynamic parameters: The influence of corrosion rate on temperature can express by Arrhenius calculation

$$k_{corr} = A\, e^{-E_a^*/RT} \quad (4)$$

Where A = pre-exponential factor and Ea^* = activation energy. A plan between log (k_{corr}) of SS 430 in attendance and lack of altered dose of FH extract and the (1/T) is displayed **in Fig (3**) Ea^* can be gotten from slope of these lines. The measured data summarized in **Table (3**). The data of E_a^* for hindrance solution is greater than that for unhindered solution, suggest that liquefaction of FH extract decreases due to the creation of film of the extract on surface of SS430 [18-19]. ΔH^* and ΔS^* of the corrosion manner were measured from the transition state equation 5.

$$k_{corr} = \frac{RT}{Nh}\, e^{\Delta S^*/R}\, e^{-\Delta H^*/RT} \quad (5)$$

Where, h = Planck's constant. A plan of 1/ T vs log (k_{corr}/T) for SS430 in 2 M HCl with an altered dose of FH extract obtain lines straight as displayed in **Figure (4)** Calculated values listed in **Table (3),** The sign of ΔH^* data was positive. That suggests that the endothermic process, and negative values of ΔS^* meaning that there is a decrease in disorder occur during progression of the transition from reactants to the activated complex[20].

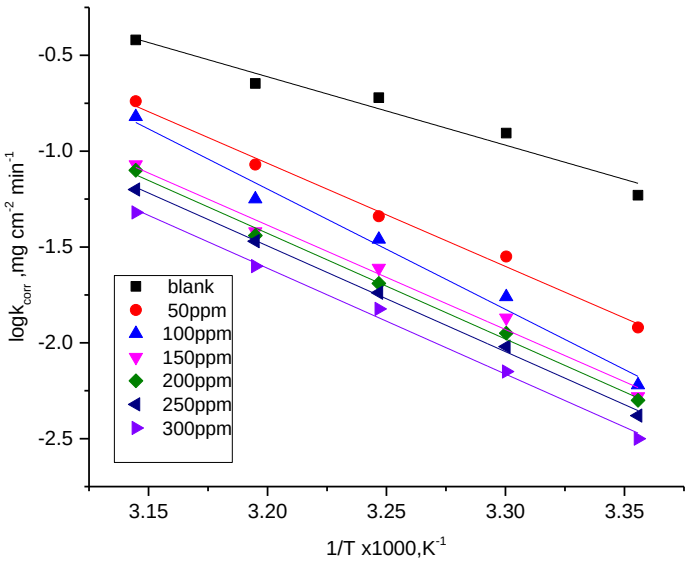

Fig (3): log (k_{corr}) vs. 1/T of SS430 corrosion in 2M HCl without and with various doses of FH extract

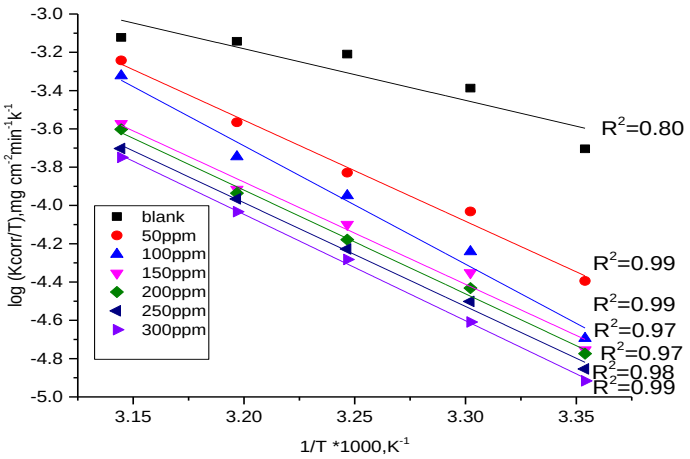

Fig (4): (log k_{corr} / T) vs. 1/ T for corrosion of SS430 in 2M HCl without and with various concentrations of FH extract

Table (3): Activation parameters obtained for corrosion of SS430 without and with various doses of FH extract

Conc, ppm	**E^*_a kJ mol^{-1}**	**ΔH^* kJ mol^{-1}**	**$-\Delta S^*$ J mol^{-1}K^{-1}**
Blank	68.3	51.48	93.3
50	103.0	100.0	57.8
100	103.5	101.0	56.1
150	104.1	102.2	55.1
200	105.4	103.6	59.2
250	105.6	103.7	58.0
300	105.7	106.3	64.7

3.4 Electrochemical measurements

3.4.1 EIS tests: Figs. (5 & 6) Demonstrations Nyquist, and bode diagrams gotten from EIS test for SS430 in 2.0 M HCl in the existence of various doses (50-300) ppm of the FH extract correspondingly. The breadth of Nyquist diagrams rises with increasing FH extract dose, which implies a promotion of inhibitory effect. Nyquist plot consists of depressed semicircle due to the roughness of SS430 surface and inhomogeneities of metal electrodes. The circuit correspondent to outcome data is displayed in the Fig. (7). The capacitance double layer (C_{dl}) and % IE were calculated using equations (6) and (7), respectively

$$C_{dl} = \frac{1}{2\pi f_{max} R_{ct}} \quad (6)$$

Where, f_{max} is the maximum frequency at which the imaginary constituent of the impedance (Z_{im}) is higher

$$\%IE = \frac{R_{ct} - R^{\circ}_{ct}}{R_{ct}} \quad (7)$$

Where, R_{ct} and R^{0}_{ct} are the resistance existence and nonexistence FH extract, correspondingly.

Extracted parameters have represented in Table (4). From Table (4) we found that R_{ct} improve with improving concentration of FH extract, demonstrating the lower in corrosion rate of SS430 in attendance of FH extract. Moreover, The Capacitance double layer value decreases with increase of FH extract concentration due to replacement of water molecules by FH molecules.

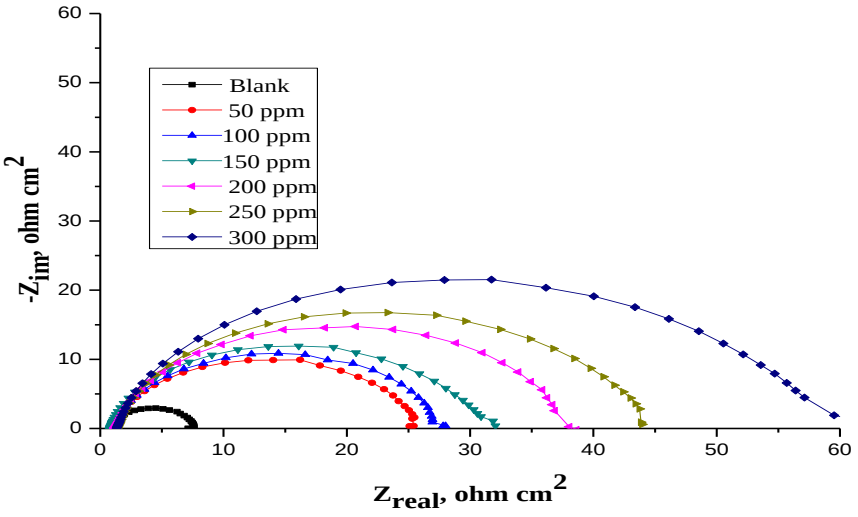

Fig (5): EIS Nyquist diagrams for SS 430 in 2 M HCl without and with various doses of FH extract

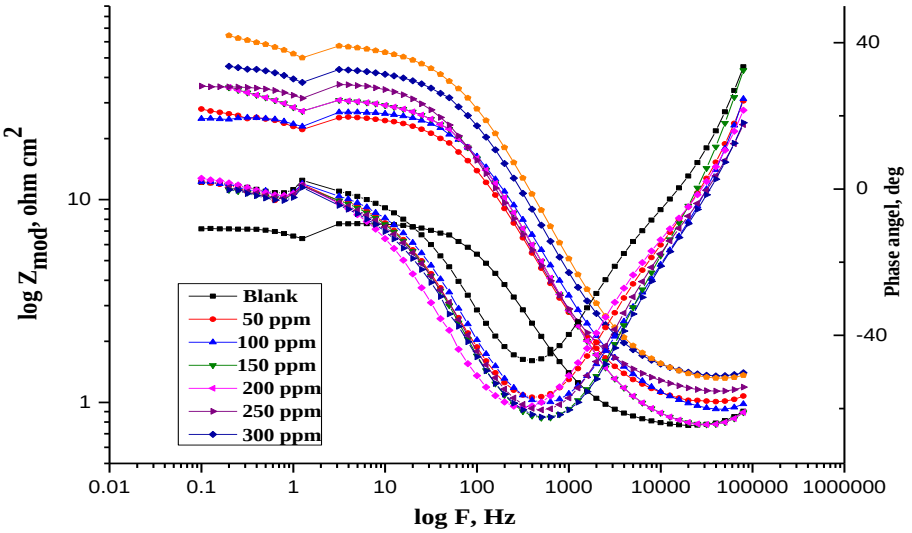

Fig (6): EIS Bode diagrams for SS 430 in 2 M HCl in the existence and nonexistence of altered dose of Ferula hermonis.

Table (4): EIS value of SS430 in 2 M HCl and with and without different dose of FH extract at 25 ºC

[inh.],ppm ppm	R_{ct}, Ω cm^{-2}	C_{dl}, µFcm^{-2}	θ	%IE
0.0	6.458	197	----	---
50	12.71	91.6	0.492	49.2
100	25.11	79.5	0.743	74.3
150	35.02	68.8	0.816	81.6
200	38.37	63.2	0.832	83.2
250	52.18	54.7	0.876	87.6
300	55.54	47.1	0.884	88.4

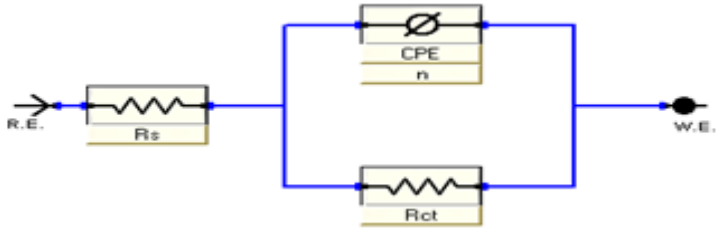

Fig (7) Equivalent circuit utilized to fit the EIS data

3.4.2 PP tests: PP diagrams of SS430 in 2.0M HCl in the existence and nonexistence of altered dose of FH extract presented in Fig (8). The parameters obtained from PP technique such as (E_{corr}), (I_{corr}), (β_a) and (β_c) deduced from the curves are given in Table (5). I_{corr} determined by Tafel extrapolation can utilize to measure of %IE through the following equation

$$\%IE = \frac{I_{corr} - I_{corr(inh)}}{I_{corr}} \quad (8)$$

Where I_{corr} and $I_{corr(inh)}$ are the current existence and nonexistence FH extract, correspondingly.

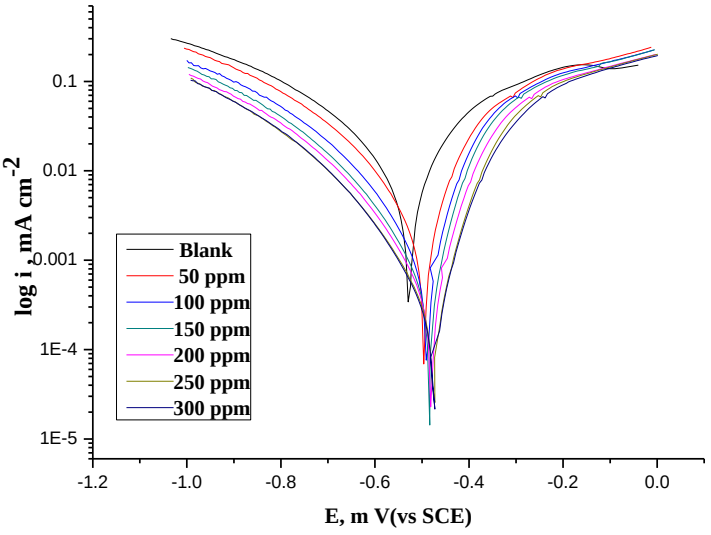

.

Fig. (8): PP diagrams for the liquefaction of SS 430 in 2.0 M HCl in the existence and nonexistence of altered dose of Ferula hermonis at 25ºC.

Table 5: Parameters gotten from PP technique containing various concentrations of FH extract at 25 ºC

[inh.] ppm	- $E_{corr,}$ mV(vs.SCE)	$i_{corr,}$ µA cm^{-2}	β_c mV dec^{-1}	β_a mV dec^{-1}	Θ	% IE
Blank	527	4770	150.6	107	----	----
50	495	1440	122.7	72	0.698	69.8
100	489	744	123.9	63	0.844	84.4
150	484	439	116.4	57	0.907	90.7
200	480	323	110.9	57	0.932	93.2
250	475	243	120.2	62	0.949	94.9
300	475	164	98.3	54	0.965	96.5

It seen that from **Table 5,** both anodic and cathodic reactions are influence in attendance of ferula hermonis extract, also the shift in E_{corr} towards negative direction but is small than 85 mV suggest that ferula hermonis act as mixed kind inhibitor[21]. Addition of ferula hermonis extract suppresses I_{corr} and this cause an increase in inhibition efficiency reached 96.5% in existence of 300 ppm of ferula hermonis.

3.4.3 EFM tests: EFM technique for the corrosion of SS430 in 2 M HCl without and with various doses of FH extract have presented in **Fig (9).**

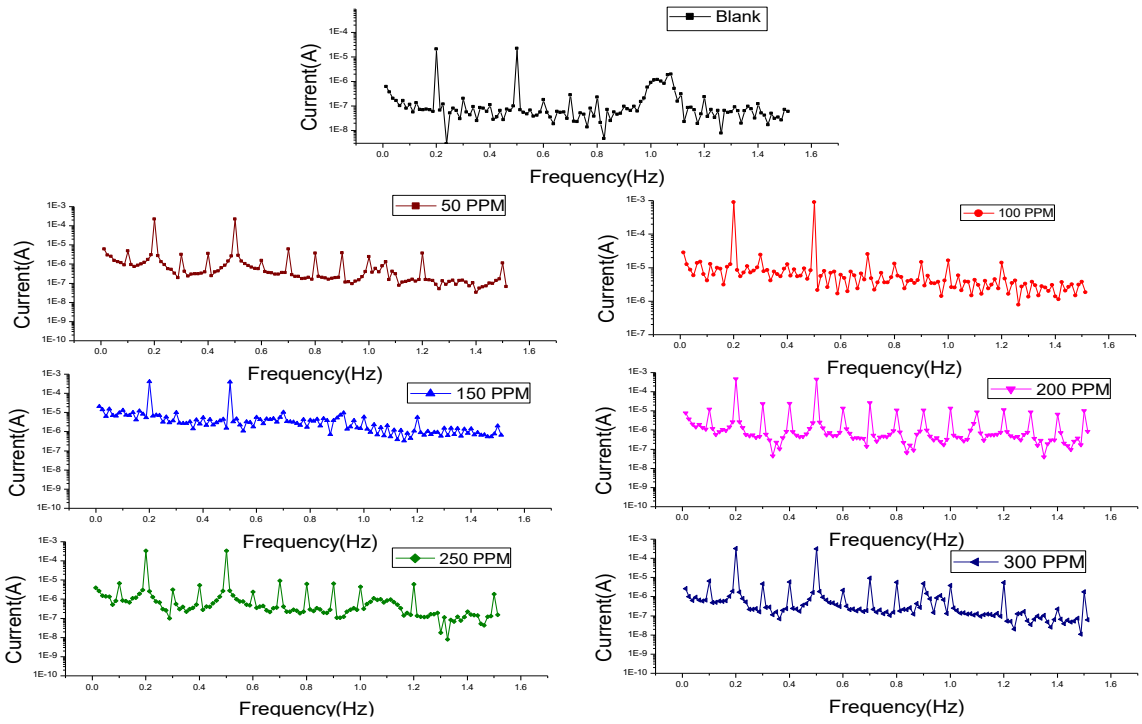

Fig. (9): EFM data obtained from dissolution of SS430 in 2 M HCl solution without and with various doses of FH extract

The maximum peaks utilized to measure the parameters such as causality factors (CF-2, CF-3), I_{corr}, (β_a, β_c) and %IE without and with FH extract, and the data are summarized in Table (6), it is observed that I_{corr} data lower with rise dose of FH various conditions are equal to the data obtained from theoretical confirm that calculated data are confirmed and of excellent quality[22].

Table (6): Parameters obtained from EFM test for the corrosion of SS430 in 2 M HCl solution in presence of various doses of FH extract at 25°C

Conc. ppm	i_{corr} , µA cm^2	β_a, mV dec^{-1}	β_c, mVdec^{-1}	CF-2	CF-3	C.R. mpy	θ	%IE
Blank	3788	101	116	1.9	3.0	1731		
50	548.9	82	94	1.8	1.8	250	0.855	85.5
100	537.8	66	85	1.4	2.1	245	0.858	85.8
150	439.8	80	88	1.3	2.9	200	0.884	88.4
200	432	82	93	1.6	2.8	197	0.886	88.6
250	315.9	81	89	1.4	3.1	144	0.917	91.7
300	295.3	82	91	1.5	03.	135	0.922	92.2

3.5 Surface characterization

3.5.1 SEM analyses: SEM micrographs obtained for SS 430 samples without and with 300 ppm of the FH extract after exposure for 15h immersion are shown in **Fig (10).** It is very clear that polished SS430 surface suffers from huge damage in the presence of the corrosive medium. This damage decreased in the presence of FH extract. This can regarded to formation of passive film through adsorption of the extract on SS430 surface blocking the active center.

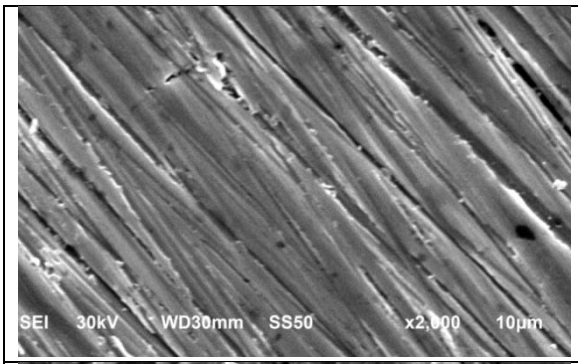

(a) polished SS430

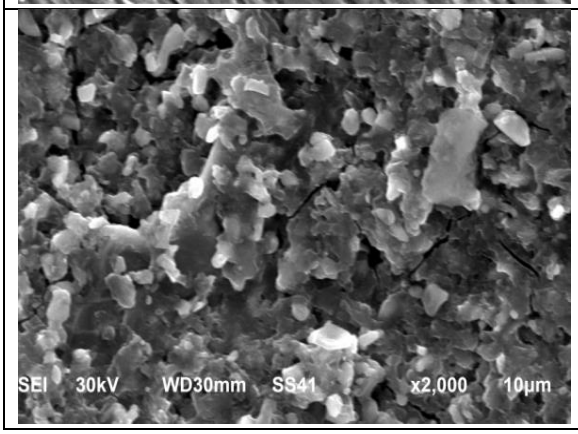

(b) blank 2M HCl

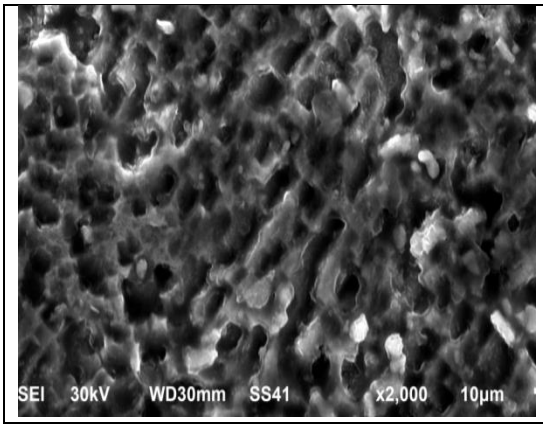	(c)SS430+FH extract

Fig (10): SEM images of (a) polished SS430 (b) after 15 h immersion in 2 M HCl and (c) after 15 h immersion in 2 M HCl + 300 ppm of FH extract

3.5. AFM examination: The surface roughness of SS430 immersion in 2M HCl without and with 300 ppm of FH extract has evaluated by AFM. Fig (11) (a) shows polished SS430 where, (b) SS430 in 2M HCl and (c) SS430 in 2M HCl with 300ppm FH extract. The area and line roughness are listed in Table (7). The roughness rise in existence of HCl because of the corrosion of SS430 but in the attendance of the FH extract the roughness was breakdown due to ferula hermonis adsorbed on SS430 forming shielding layer, lead to that surface of SS430 became more smoothly.

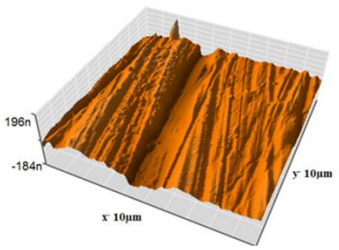	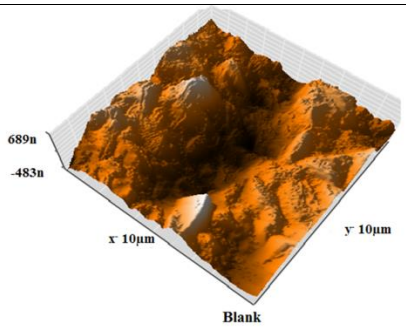	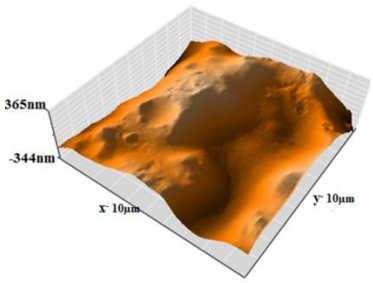
(a) polished SS430	(b) SS430 in 2M HCl	(c) SS430+ ferula hermonis

Fig (11) (a): 3D AFM image of SS430 free surface (b) 3D AFM image of SS430 after inundation in 2M HCl for 15 h (c) 3D AFM after 15h immersion in 2MHCl +300 ppm FH extract

Table (7): AFM parameters for SS430 in 2M HCl without and with 300 ppm FH extract

Parameters	polished SS430	SS430 in 2MHCl	SS430 in 2M HCl+300 ppm FH extract
The roughness average (Sa)	18.52	174.18	95.279
The mean value (Sm)	-10.246	-13.269	-11.795
The root mean square (Sq)	25.156	210.89	115.92
The valley depth (Sv)	-93.343	-560.59	-523.32
The peak height (Sp)	162.29	1332.3	217.23
The peak-valley height (Sy)	255.63	1892.7	740.54

3.5.3 Fourier transforms infrared spectroscopy (FT-IR): Spectra of stock the FH extract and SS430 surface after immersion in 2M HCl +300 ppm of the extract for 3 hours at 25° c has presented in Fig (12).It is obviously clear that all bands of FH extract observed on SS430 surface with low intensity and small shift. The peaks parallel to OH at 3380 cm^{-1} shifted to3358 $cm^{-1}$and the peaks attributed to C-H stretch at 2971 cm^{-1} shift to 2960 cm^{-1},and the peaks of C=O stretch at 1668 cm^{-1}showd shift at 1637 cm^{-1}, and the peaks of C-H at 1436 cm^{-1}showd shift at 1428 cm^{-1} which cross bonding to methyl group. This means that FH extract is completely adsorbed on the SS 430 surface. And the shifted peaks can be assigned to the interaction of adsorbed inhibitor molecules to metal surface

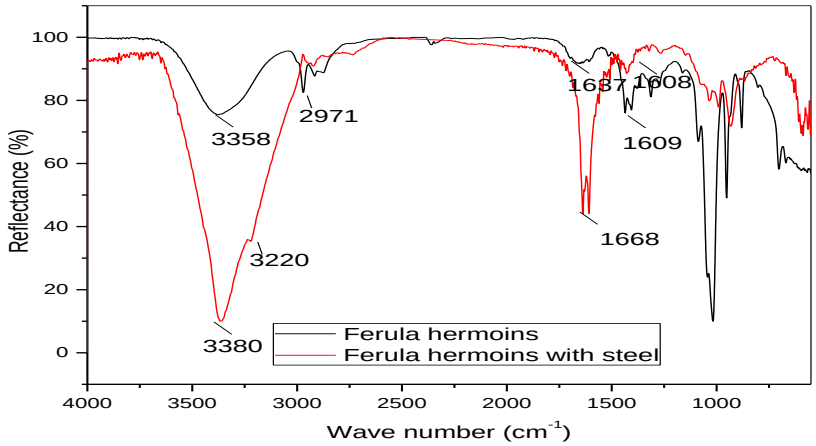

Fig. (12): FTIR spectra of the FH extract of stock solution and adsorbed layer of FH on SS430 surface

3.6. Mechanism of corrosion inhibition: Adsorption of FH extract can be clarified on the basis that adsorption of the inhibitor was mostly via hetero atoms (viz., N) exist in various constituents of the FH extract in attaching to the accessibility of π- electrons in the aromatic ring [23]. The phytochemical components present in the FH extracts contain many active sites such as S, O and N, which are regarded as centers of adsorption.

CONCLUSIONS

FH extract has tested as green corrosion inhibitors for SS430 and give the best inhibition efficiency 94.5% at 300 ppm based on weight loss measurements. Polarization study ensures that FH extract act as a mixed kind inhibitor, while the EIS study showed that R_{ct} rise with increasing FH extract concentration and capacitance double layer decreased, suggesting that FH extract hindrance corrosion by adsorption mechanism, and adsorption follow Langmuir isotherm.

REFERENCES

1. L.Shreir, R. Jarman, and G. Burstein, *Corrosion, volume 1, Metal/Enviroment Reaction*, 1994, Butterworth Heinemann.
2. A.A.Hermas , M.S. Morad, M.H.Wahdan, Effect of PgTPhPBr on electrochemical corrosion behavior of 304 SSin H2SO4 solution .J. Appl. Elecreochem. 2004.**34**: p.95-102.
3. S.Deng and X. Li, Inhibition by Ginkgo leaves extract of the corrosion of steel in HCl and H2SO4 solutions. Corrosion Science, 2012. **55**: p. 407-415.

4. G.Ji , S. Anjum, S.Sundaram, R. Prakash, Musa paradisica peel extract as green corrosion inhibitor for mild steel in HCl solution. Corrosion Science, 2015. **90**: p. 107-117.
5. N.Odewunmi, S. Umoren, and Z. Gasem, Utilization of watermelon rind extract as a green corrosion inhibitor for mild steel in acidic media. Journal of Industrial and Engineering Chemistry, 2015. **21**: p. 239-247.
6. S.Hooshmand Zaferani , M.Sharifi , D. Zaarei, M. Reza Shishesaz, Application of eco-friendly products as corrosion inhibitors for metals in acid pickling processes–A review. Journal of Environmental Chemical Engineering, 2013. **1**(4): p. 652-657.
7. A.Saxena, D. Prasad, and R. Haldhar, Use of Butea monosperma Extract as Green Corrosion Inhibitor for Mild Steel in 0.5 M H_2SO_4. Int. J. Electrochem. Sci, 2017. **12**: p. 8793-8805.
8. D. I. Njoku, I. Ukaga, O. B. Ikenna, E. E. Oguzie, K. L. Oguzie, N., Natural products for materials protection: Corrosion protection of aluminium in hydrochloric acid by Kola nitida extract. Journal of Molecular Liquids, 2016. **219**: p. 417-424.
9. I.H.Ali and M.H. Suleiman, Effect of Acid Extract of Leaves of Juniperus procera on Corrosion Inhibition of Carbon Steel in HCl Solutions. Int. J. Electrochem. Sci, 2018. **13**: p. 3910-3922.
10. A.Peimani, M. Nasr-Esfahani, Application of anise extract for corrosion inhibition of carbon steel in CO 2 saturated 3.0% NaCl solution. Protection of Metals and Physical Chemistry of Surfaces, 2018: p. 1-13.
11. M. Abdallah Hatem M. Altass, B. A. AL Jahdaly and M. M. Salem, Some natural aqueous extracts of plants as green inhibitor for carbon steel corrosion in 0.5 M sulfuric acid. Green Chemistry Letters and Reviews, 2018. **11**(3): p. 189-196.
12. Ladislav Vrsalović, Senka Gudić, David Gracić, Ivana Smoljko, Ivana Ivanić, Maja Kliškić, Emeka E. Oguzie,. Corrosion Protection of Copper in Sodium Chloride Solution using Propolis. International Journal of Electrchemical Science, 2018. **13**(1): p. 2102-2117.
13. M.Shahidi Zandi, G. Golestani, and M.R. Gholamhosseinzadeh, Mentha spicata L. extract as a green corrosion inhibitor for carbon steel in HCl solution. Physical Chemistry Research, 2017. **5**(2): p. 293-307.
14. O.John Wisdom, Denkoro Kelechi, Joseph Ugochukwu, Green Inhibitor for Corrosion of Aluminium Alloy AA8011A in Acidic Environment, International Research Journal of Engineering and Technology (IRJET), 2018. **5** (2): p.121-124.
15. S.Umoren and U. Ekanem, Inhibition of mild steel corrosion in H2SO4 using exudate gum from Pachylobus edulis and synergistic potassium halide additives. Chemical Engineering Communications, 2010. **197**(10): p. 1339-1356.
16. I. Zaafarany and M. Abdallah, Ethoxylated fatty amide as corrosion inhibitors for carbon steel in hydrochloric acid solution. Int J Electrochem Sci, 2010. **5**: p. 18-28.
17. A.Döner and G. Kardaş, *N*-Aminorhodanine as an effective corrosion inhibitor for mild steel in 0.5 M H2SO4. Corrosion Science, 2011. **53**(12): p. 4223-4232.
18. M.N. El-Din, and E. Khamis, Utilization of sulfidated poly (acrylamide-vinyl acetate) as a new corrosion inhibitor for carbon steel in acidic media. Journal of Industrial and Engineering Chemistry, 2015. 24: p. 342-350.

19. K.Ansari. and M. Quraishi, Experimental and quantum chemical evaluation of Schiff bases of isatin as a new and green corrosion inhibitors for mild steel in 20% H2SO4. Journal of the Taiwan Institute of Chemical Engineers, 2015. 54: p. 145-154.
20. V.R.Saliyan, and A.V. Adhikari, Inhibition of corrosion of mild steel in acid media by N′-benzylidene-3-(quinolin-4-ylthio) propanohydrazide. Bulletin of Materials Science,., 31(4)(2008): p.699-711
21. A.A.Nazeer, H. El-Abbasy, and A. Fouda, Adsorption and corrosion inhibition behavior of carbon steel by cefoperazone as eco-friendly inhibitor in HCl. Journal of materials engineering and performance, 2013. 22(8): p. 2314-2322.
22. Gamry Echem Analyst Manual ,2003.
23. K.F.Khaled, Molecular simulation, quantum chemical calculations and electrochemical studies for inhibition of mild steel by triazoles Electrochim. Acta, 2008, 53(9), p. 3484-3492

Corresponding author: A.S.Fouda

Chemistry Department, Faculty of Science, Mansoura University, Mansoura-35516, Egypt,

Online publication Date: 16.06.2017